

3D high-resolution imaging of lithospheric V_P , V_S , and density structure in the Alps using full-waveform inversion of the teleseismic P waves

Najmieh Mohammadi¹ Stephen Beller¹ Vadim Monteiller² and Stéphane Operto¹

¹GeoAzur, CNRS, Université Côte d'Azur

²Laboratoire de Mécanique et d'Acoustique, CNRS, Université Aix Marseille



Introduction

The convergence between the African and European plates lead to the complicated geological structure beneath the Alpine chain. Despite numerous studies on the Alpine lithosphere, many topics, such as the crustal structure beneath the Alps-Apennines junction, the geometries, orientations, and fates of the Alpine and Apennine slabs, etc. are still under debate. The high-resolution model Investigations of the crust and upper mantle simultaneously can provide a better understanding of the geodynamic process controlling the evolution of the Alps. For this purpose, we apply the method of Full Waveform Inversion (FWI) on the 203 teleseismic earthquakes recorded by 1232 stations including permanent seismological broadband stations and the AlpArray temporary seismic network. In this poster, we show a preliminary FWI result obtained by using 17 events. This benchmark elastic models of V_P , V_S , and density help us to check the data quality control process and to improve the method.

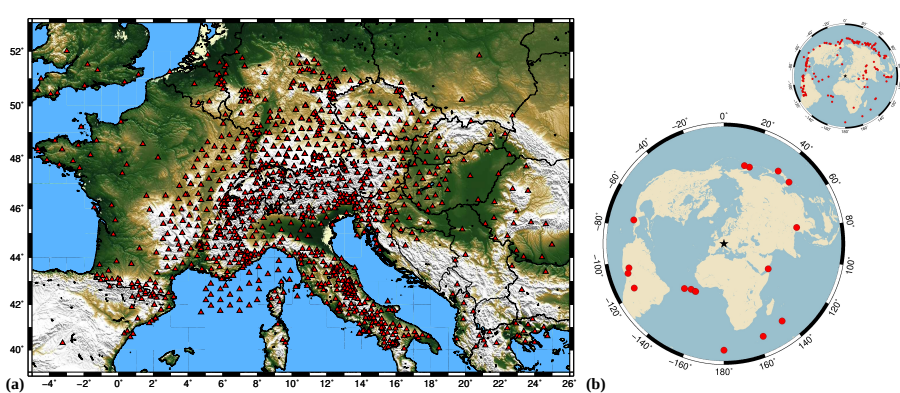


Figure: (a) Location map of the broadband stations shown by the red triangles. (b) Map showing the global distribution of the selected 17 teleseismic events and all events used in the study.

Data Processing

- First, we used a semi-automated data pre-processing method designed to make a high-quality data bank by checking the amplitude (statistical analysis, coherency test, ...), phase, and travel time of seismograms and removing those that are out of range.
- Second, we compared the observed and synthetic seismograms computed by AxiSEM [3]. We estimated synthetics according to the observed data information and used AK135 global velocity model as the initial model. In the next step, we estimated initial synthetics by convolution of the synthetics and source signatures.

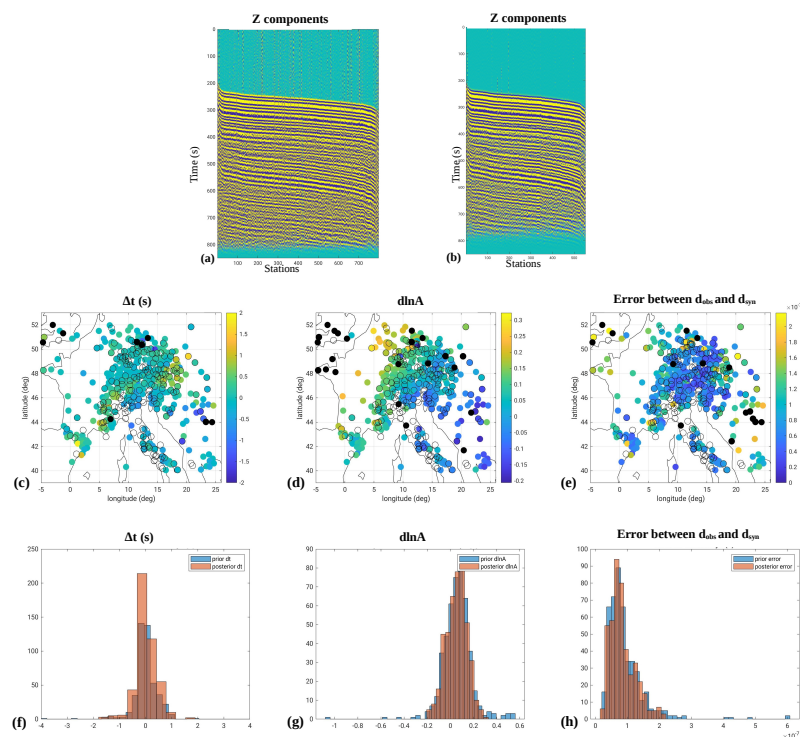


Figure: ((a) shows the Z component seismograms of all stations recorded the 2017-09-08 earthquake. (b) shows the Z component seismograms after excluding the bad-quality data. (c) shows the time misfit between the observed and synthetic seismograms. The empty black circles show stations were removed in pre-processing and the black filled ones were removed because of unaccepted delay time. (d) shows the amplitude misfits of the observed and synthetic seismograms. (e) shows the waveform misfits of the observed and synthetic seismograms. (f-h) show the binned histograms of the time, amplitude, and waveform misfits, respectively.

FWI and experimental set up

- FWI minimizes the misfit between the entire recorded and synthetic seismograms iteratively to reconstruct multiparameter models of the Earth's interior with a resolution close to the wavelength. In teleseismic FWI, sources are far away from receivers and the wavefield can be approximated by an incident nearly planar wavefield incoming from outside of the lithospheric target.
- Forward modeling is computed based on the hybrid technique [2] in two steps to decrease the computational cost of high-frequency simulations. First, the global wavefields from the source to the boundaries of the study domain are computed once with AxiSEM, then injected locally into the lithospheric target with SPECSEM3D-Cartesian at each simulation of the inverse problem.

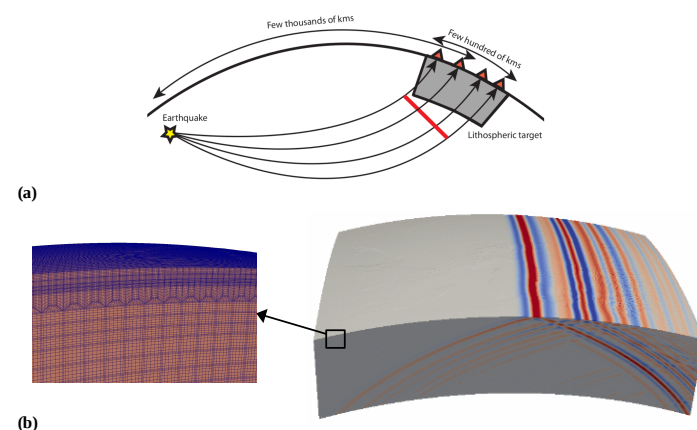


Figure: (a) propagation of the teleseismic waves. (b) Synthetic propagation of wavefield beneath the study area

- The target lithospheric mesh is centered at $lat=46^\circ$ and $lon=10^\circ$ extended over 30×20 degrees and down to 750 km depth. The element size varies from 20 km in the crust to 60 km in the mantle. The mesh contains 146520 (P8) hexahedral elements and a total of 51350682 degrees of freedom.
- We used the smoothed 1D AK135 as the initial model and filtered the time windowed (25 s before and 25s after P-onset) P-wave seismograms in a period band of 10 to 25s.
- The Laplace filter with coherent of $L_z = 25km, L_x = L_y = 50km$ was applied on the gradient. We optimize the inverse problem with the limited-memory BFGS optimization algorithm.

Resolution analysis

- The spatial resolution of the FWI is mainly controlled by two factors: the limited bandwidth of the source and the limited spread of the acquisition. To check the resolution power and acquisition setup, we designed a synthetic test by superimposing the inclusions with a radius of 30 km onto the initial model at different positions and depths. The parameters of the inclusions have been perturbed $\pm 10\%$ with respect to the background model.

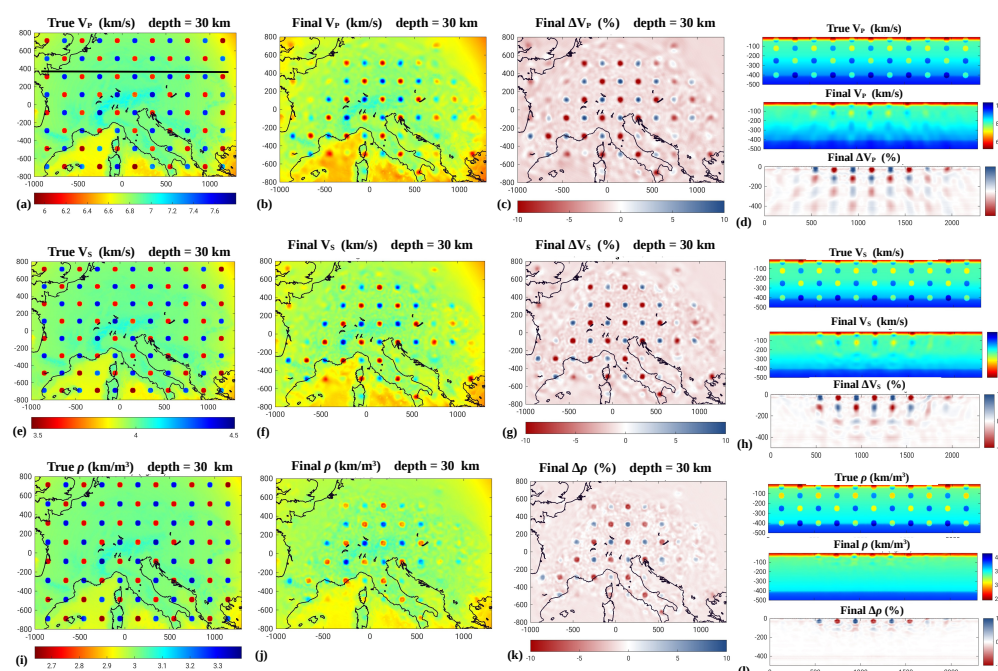


Figure: V_P , V_S , and ρ resolution analysis. (a-c) show depth slices of the true synthetic V_P , the final V_P , and perturbations of the final V_P , respectively. (d-f) show depth slices of the true synthetic V_S , the final V_S , and perturbations of the final V_S , respectively. (g-i) show depth slices of the true synthetic ρ , the final ρ , and perturbations of the final ρ , respectively. (j, h, and i) show vertical slices of resolution tests along the profile shown by the black line on (a) for V_P , V_S and ρ , respectively.

Resolution analysis

- The reconstructed depth slice at 30 km depth shows that there are no significant aliasing artifacts.
- The lower resolution of the V_P than V_S is due to the longer wavelength of P in comparison with S. V_P model reconstruction also benefits from PP transmitted wave in contrary to the V_S model that benefits from the converted PS wave in the forward-scattering mode.
- At higher depths, the density perturbations, depending on the amplitude of the waveform, decrease rapidly. This parameter is more sensitive to the back-scattering of the reflected PP and PS waves [1] that have weak amplitudes and become weaker when depth increases.

Preliminary FWI model for V_P , V_S , and ρ

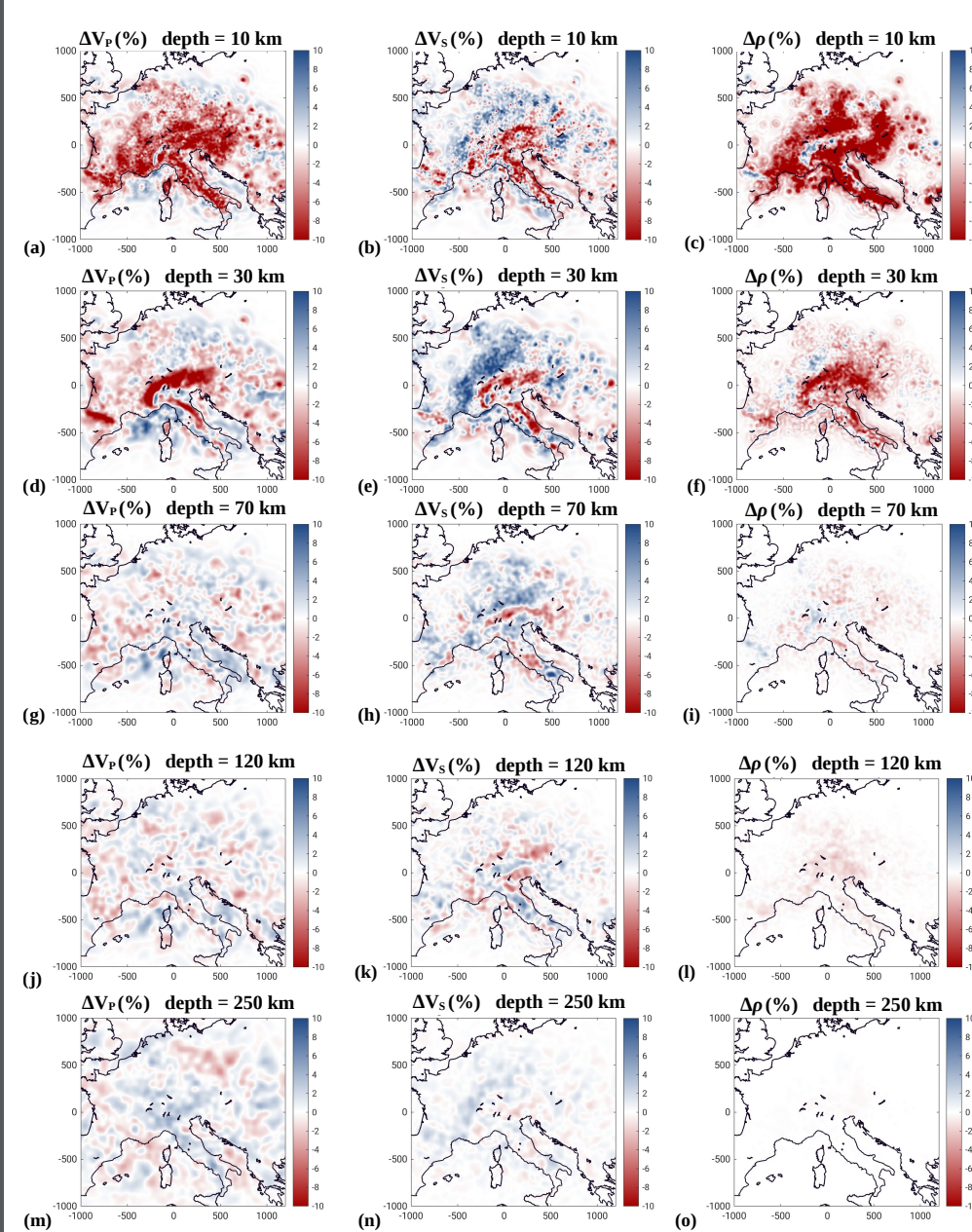


Figure: V_P , V_S and ρ perturbations at depths of 10, 30, 70, 120, and 250 km.

- The isotropic V_P , V_S , and ρ models are shown in the above figure. We see that the main structures such as the Pyrenees, and the high-velocity of the Ivrea body were resolved with a good resolution at depths less than 70 km for all three parameters. The low velocity of the V_P model at depth of 10 km matches the thick sediment in the Pô plain, the foreland molasse basin, and the Rhône-Bresse graben. In the depth of 30 km, V_P , V_S , and ρ models show lower perturbations in the Alpine domain and the Northern Apennines confirming deeper Moho in these regions.

- We also compared the vertical sections of the FWI for V_P and V_S with the work of Paffrath et al (2021). We see that FWI by using only 17 events could retrieve the most features revealed by teleseismic P-wave tomography. In both V_P and V_S sections, we can see that the high-velocity anomaly of the Adriatic lithosphere has been recovered. This high-velocity model becomes deeper in the V_P model and can be related to the Dinaric slab [4].

Preliminary FWI model for V_P , V_S , and ρ

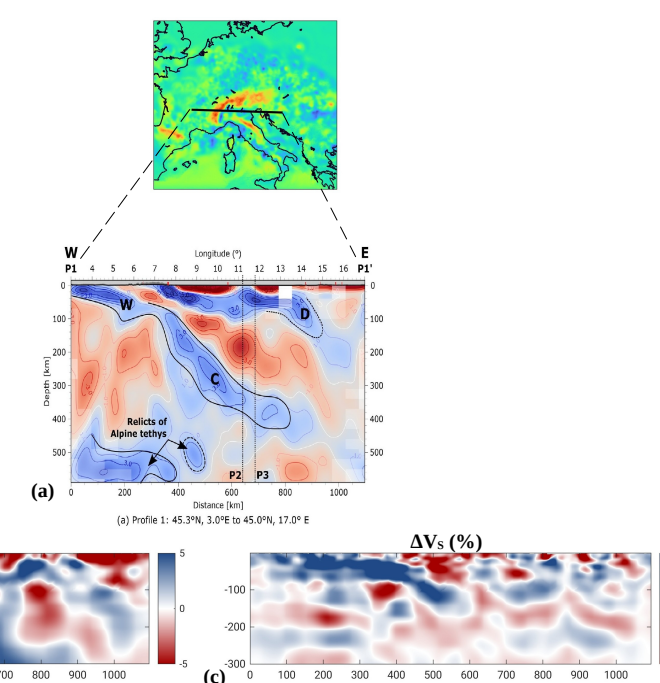


Figure: A comparison between the vertical slices of the V_P and V_S perturbations obtained by the FWI and the work of Paffrath et al. (2021). (a) shows the location of the profile and perturbation of the V_P model obtained by P-wave travel-time tomography. (b-c) shows the perturbations of V_P and V_S models obtained in this study.

- The high velocity extending from the west to beneath the Penninic Front shown by travel time tomography has been recovered by V_S model better than the V_P model that can be reasoned by the higher resolution of the V_S because of higher wavenumber. In the V_P model, this anomaly has been covered by a horizontal strip feature that may result from the back-scattering in the updated model. One main factor of this effect is the error in the earthquake depth and CMT solution.

Conclusion

- We estimated a preliminary isotropic elastic FWI model beneath the Alpine orogen by using low-frequency P-waves. The benchmark model helps us to have better control over data selection. We could investigate the imprint of the events with error in-depth and CMT solution and exclude them from the big dataset.
- The resolution analysis shows that the acquisition footprint is not significant. In the next step, we will build the FWI model by using the whole of the P-wave dataset and also involve S and SKS phases in FWI to increase resolution by adding SP and SS scattering modes.

References

- Beller, S., Monteiller, V., Combe, L., Operto, S., and Nolet, G. (2018). On the sensitivity of teleseismic full-waveform inversion to earth parametrization, initial model and acquisition design. *Geophysical Journal International*, 212(2):1344–1368.
- Monteiller, V., Beller, S., Plazolles, B., and Chevrot, S. (2020). On the validity of the planar wave approximation to compute synthetic seismograms of teleseismic body waves in a 3-D regional model. *Geophysical Journal International*, 224(3):2060–2076.
- Nissen-Meyer, T., van Driel, M., Stähler, S. C., Hosseini, K., Hempel, S., Auer, L., Colombi, A., and Fournier, A. (2014). Axisem: broadband 3-d seismic wavefields in axisymmetric media. *Solid Earth*, 5(1):425–445.
- Paffrath, M., Friederich, W., Schmid, S. M., Handy, M. R., AlpArray, Group, A.-S. D. W., et al. (2021). Imaging structure and geometry of slabs in the greater alpine area—a p-wave travel-time tomography using alparray seismic network data. *Solid Earth*, 12(11):2671–2702.